State Estimation of Linear Systems over a Network subject to Sporadic Measurements, Delays, and Clock Mismatches

Marcello Guarro * **Francesco Ferrante** ** **Ricardo Sanfelice** *

* *Department of Computer Engineering University of California, Santa Cruz, CA 95060 USA. (e-mail: mguarro@soe.ucsc.edu, ricardo@ucsc.edu)*
** *Univ. Grenoble Alpes, CNRS, GIPSA-lab, F-38000 Grenoble (e-mail: francesco.ferrante@gipsa-lab.fr)*

Abstract: This paper proposes a hybrid observer for the estimation of the state of a plant over a realistic network. The network provides delayed measurements of the output of the plant at time instants that are not necessarily periodic and are accompanied by timestamps provided by a clock that eventually synchronizes with the clock of the observer. The proposed observer, along with the plant and communication network, are modeled by a hybrid dynamical system that has two timers, a logic variable, and two memory states to capture the mechanisms involved in the events associated with sampling and arrival of information, as well as the logic in the estimation algorithm. The hybrid model also includes a generic clock synchronization scheme to cope with a mismatch between the clocks at the plant and the observer. Convergence properties of the estimation error of the system are shown analytically and supported by numerical examples.

Keywords: Hybrid and switched systems modeling, Observers for linear systems, Control over networks, Systems with time-delays

1. INTRODUCTION

Digital communication networks have become ubiquitous in the fields of control systems and estimation, due to their low cost and ease of configuration. The union of these technologies has created the interdisciplinary field of Networked Control Systems (NCSs) that specifically refers to the study of distributed dynamical systems that communicate via data packets over a shared network, see Hespanha et al. (2007). The use of such networks in control system applications presents unique challenges. These challenges stem from the fact that control theorists have traditionally treated interconnections between systems as ideal, while network theorists often assume that communication channels are subject to unknown disturbances, and therefore imperfect, Hespanha et al. (2007). Network disturbances in the form of packet delays and dropouts can often degrade control system performance and may, in some cases, destabilize the system if not taken into account Zhang et al. (2001). Network disturbances are traditionally addressed by implementing network-level protocols designed to minimize such disturbances (e.g., CAN, FlexRay, TTP, etc.) to negligible levels. However, in cases were such protocols prove impracticable, a model-based design of the system that includes assumptions about network disturbances may be the only approach. This paper addresses this scenario.

Treating the system as a traditional aperiodic sampled system with regular sensor sampling intervals, despite a variable delay on its transmission, constitutes one of the model-based approaches presented in the literature for packet dropout and delay disturbances. Results on such systems have been well characterized as shown in Nesic and Teel (2004) and Montestruque and Antsaklis (2003). Of particular interest are the results that utilize hybrid systems modeling as exhibited in the works by Zhang et al. (2001), Nesic and Teel (2004), and Li and Sanfelice (2013). Jungers et al. (2017) shows a method of abstracting the time-varying delay problem as a controllability problem with packet losses. The inability to apply the aforementioned results to an NCS that has both aperiodic sampling and variable delays in the transmission of the sampled data constitutes a noted discrepancy and motivates the work in this paper. Moreover, we are not aware of any such result that considers the inclusion of a clock synchronization scheme.

This paper presents a hybrid observer for the estimation of the state of a plant over a network subject to latency delays. Measurements of the output plant are given at aperiodic time instants and incur a variable delay during their transmission. The measurements are accompanied by timestamps provided by the clock of the plant that is not synchronized with the clock of the observer. More

⋆ This research has been partially supported by the National Science Foundation under CAREER Grant no. ECS-1450484, Grant no. ECS-1710621, and Grant no. CNS-1544396, by the Air Force Office of Scientific Research under Grant no. FA9550-16-1-0015, by the Air Force Research Laboratory under Grant no. FA9453-16-1-0053, and by CITRIS and the Banatao Institute at the University of California.

specifically, building on the results in Ferrante et al. (2016), this paper introduces a hybrid system model of an NCS that possesses the ability to capture aperiodic sensor sampling with communication delays and desynchronized node clocks utilizing the framework presented in Goebel et al. (2012). Furthermore, we demonstrate the model's flexibility to implement clock synchronization schemes in the case of drifting clocks in the subsystems of an NCS and provide results for global attractivity. This paper is organized as follows: Section 2 presents the system being studied; an outline of the algorithm under consideration for the observer law; and the associated hybrid modeling of the system interconnected with the observer. Section 5 details the main results, while section 6 provides numerical examples. In particular, the IEEE 1588 clock synchronization protocol (see IEEE (2008)) is considered and analyzed within the hybrid model. Due to space constraints, the proof of the results along with other details will be published elsewhere.

Notation: In this paper the following notation and definitions will be used. $\mathbb{N}$ denotes the set of natural numbers, i.e., $\mathbb{N} = \{0, 1, 2, ..\}$. $\mathbb{N}_{>0}$ denotes the set of natural numbers not including 0, i.e., $\mathbb{N}_{>0} = \{1, 2, ..\}$. $\mathbb{R}$ denotes the set of real numbers. $\mathbb{R}_{\geq 0}$ denotes the set of non-negative real numbers, i.e., $\mathbb{R}_{\geq 0} = [0, \infty)$. $\mathbb{R}^n$ denotes n-dimensional Euclidean space. Given topological spaces A and B, $F : A \rightrightarrows B$ denotes a set-valued map from A to B. For a matrix $A \in \mathbb{R}^{n\times m}$, A^T denotes the transpose of A. Given a vector $x \in \mathbb{R}^n$, $|x|$ denotes the Euclidean norm. Given two vectors $x \in \mathbb{R}^n$ and $y \in \mathbb{R}^m$, $(x, y) = [x^\mathsf{T} \;\; y^\mathsf{T}\,]^\mathsf{T}$. Given a matrix $A \in \mathbb{R}^n$, $|A| := \max\{\sqrt{|\lambda|} : \lambda \in \text{eig}(A^\mathsf{T}A)\}$. For two symmetric matrices $A \in \mathbb{R}^n$ and $B \in \mathbb{R}^n$, $A \succ B$ means that $A - B$ is positive definite, conversely $A \prec B$ means that $A - B$ is negative definite. Given a closed set $A \subset \mathbb{R}^n$ and closed set $B \subset A$, the projection of A onto B is denoted by $\Pi_B(A)$. Given a function $f : \mathbb{R}^n \to \mathbb{R}^m$, the range of f is given by $\text{rge } f := \{y \mid \exists\, x \text{ with } y \in f(x)\}$.

2. MOTIVATIONAL EXAMPLE

In this paper, we consider linear plants given by

$$\dot{z} = Az, \qquad y = Mz \tag{1}$$

where $z \in \mathbb{R}^n$ is the state and $y \in \mathbb{R}^m$ is the output. The matrices A and M are constant and of appropriate dimensions. To reconstruct z from measurements of y, consider a networked observer receiving measurements y sampled and broadcast at times t_k, $k \in \mathcal{I}_m$, $k > 0$ where $\mathcal{I}_m := \{2i + 1 : i \in \mathbb{N}\}$. Moreover, the network experiences varying transmission delays such that the measurements $y(t_k)$ are available only at times t_k, $k \in \mathcal{I}_d$, $k > 0$, where $\mathcal{I}_d := \{2i : i \in \mathbb{N}\}$. The resulting sequence of times $\{t_k\}_{k=0}^{\infty}$ capturing the sampling and arrival of the measurements are described by a strictly nondecreasing unbounded sequence of instants $\{t_k\}_{k=0}^{\infty}$ with $t_0 = 0$. Following Ferrante et al. (2016), we assume that there exist scalars $0 < T^d \leq T_1^N \leq T_2^N$ such that each such sequence satisfies

$$\begin{aligned} &0 \leq t_1 \leq T_2^N, \;\; T_1^N \leq t_k - t_{k-2} \leq T_2^N \quad \forall k \in \mathcal{I}_m, k > 0 \\ &0 \leq t_k - t_{k-1} \leq T^d \qquad\qquad\qquad\quad \forall k \in \mathcal{I}_d, k > 0 \end{aligned} \tag{2}$$

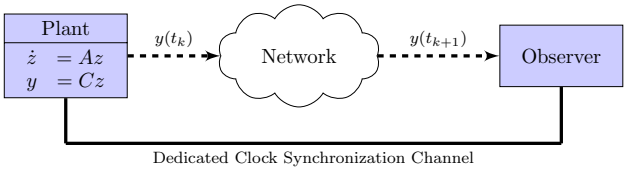

Fig. 1. Block diagram of the system.

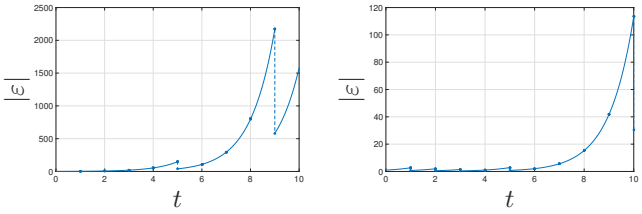

Fig. 2. The evolution of the estimation error with respect to real time for $T^d = 0.2$ (left) and $T^d = 0.02$ (right). The vertical dashes represent the resets of $\hat{z}$ according to $\hat{z}^+$.

The scalars T_1^N and T_2^N define the minimum and maximum allowable transfer interval (MATI), respectively, while T^d is an upper bound on the transmission delay.

Now, consider the impulsive observer proposed in Ferrante et al. (2016)

$$\begin{cases} \dot{\hat{z}} = A\hat{z} & \forall t \notin \{t_k\}_0^{+\infty} \\ \hat{z}(t_k^+) = \begin{cases} \hat{z}(t_k) + L(y(t_{k-1}) - M\hat{z}(t_k)) & \forall k \in \mathcal{I}_d \\ \hat{z}(t_k) & \forall k \in \mathcal{I}_m \end{cases} \end{cases} \tag{3}$$

where L is a gain matrix designed to guarantee that the estimation error $\varepsilon := z - \hat{z}$ converges to zero.

From Ferrante et al. (2016), we review the example given by the following system data: $A = 1$, $M = 1$ with chosen constants $T_1 = T_2 = 1$ and $L = 1 - e^{-1}$ designed such that the sufficient conditions in Ferrante et al. (2016), for convergence of ε to zero under the presence of delays, are satisfied. Then, let $T^d = 0.2$. Simulating the observer in (3), Figure 2 shows that the norm of the estimate error $\varepsilon = z - \hat{z}$ for the given data diverges due to the small delay introduced on the measurements. Figure 2, also shows the divergence of the estimation error for the case where $T^d = 0.02$. The observer proposed in this work solves this problem.

2.1 Proposed Observer Algorithm

Given the inability of the observer in (3) to compensate for the delays with the original observer law, we propose the following strategy:

- Measurements y broadcast at times t_k, $k \in \mathcal{I}_d$, are accompanied by a time-stamp $\ell_t(t_k) = t_k$.
- When the subsequent measurements arrive at times t_k, $k \in \mathcal{I}_m$, the current state estimate $\hat{z}(t_k)$ is backward propagated to t_{k-1}, to get
$$\hat{z}(t_{k-1}) = e^{-A\delta_k}\hat{z}(t_k)$$
where $\delta_k = t_k - \ell_t(t_{k-1})$.
- With the estimate $\hat{z}(t_k)$ retrieved, the reset law in Ferrante et al. (2014) is applied to $\hat{z}(t_{k-1})$, leading to the auxiliary quantity

$$\hat{z}^*(t_{k-1}^+) = \hat{z}(t_{k-1}) + L\big(y(t_{k-1}) - M\hat{z}(t_{k-1})\big)$$
$$= e^{-A\delta_k}\hat{z}(t_k) + L\big(y(t_{k-1}) - Me^{-A\delta_k}\hat{z}(t_k)\big)$$

- The quantity $\hat{z}^*(t_{k-1}^+)$ is then propagated forward in time, up to t_k via
$$\hat{z}^*(t_k) = e^{A\delta_k}\hat{z}^*(t_{k-1}^+)$$
$$= \hat{z}(t_k) + e^{A\delta_k}L\big(y(t_{k-1}) - Me^{-A\delta_k}\hat{z}(t_k)\big)$$
which is the actual quantity that $\hat{z}$ is reset to.

Note that the associated clock synchronization scheme to ensure synchronized plant and observer clocks for the propagation of the state estimate is done separately. Thus, the proposed hybrid observer law can be summarized as follows:

$$\begin{cases} \dot{\hat{z}} = A\hat{z} & \forall t \notin \{t_k\}_0^\infty \\ \hat{z}(t_k^+) = \begin{cases} \hat{z}(t_k) + e^{A\delta_k}L\big(y(t_{k-1}) - Me^{-A\delta_k}\hat{z}(t_k)\big) & \forall k \in \mathcal{I}_d \\ \hat{z}(t_k) & \forall k \in \mathcal{I}_m \end{cases} \end{cases} \tag{4}$$

3. PRELIMINARIES ON HYBRID SYSTEMS

The continuous and discrete nature of the system under consideration is an ideal candidate for the hybrid systems modeling framework in Goebel et al. (2012). We recall that a hybrid system $\mathcal{H}$ in $\mathbb{R}^n$ is composed by the following *data*: a set $C \subset \mathbb{R}^n$, called the flow set; a set-valued mapping $F : \mathbb{R}^n \rightrightarrows \mathbb{R}^n$ with $C \subset \text{dom } F$, called the flow map; a set $D \subset \mathbb{R}^n$, called the jump set; a set-valued mapping $G : \mathbb{R}^n \rightrightarrows \mathbb{R}^n$ with $D \subset \text{dom } G$, called the jump map; Then a hybrid system $\mathcal{H} := (C, F, D, G)$ written in its compact form is given by

$$\mathcal{H} \begin{cases} \dot{x} \in F(x) & x \in C \\ x^+ \in G(x) & x \in D \end{cases} \tag{5}$$

where x is the state vector. Solutions to hybrid systems are parameterized by (t, j) where $t \in \mathbb{R}_{\geq 0}$ defines ordinary time and $j \in \mathbb{N}$ defines the jump time. The evolution of ϕ is described by a *hybrid arc* on a *hybrid time domain* Goebel et al. (2012). A hybrid time domain is given by dom $\phi \subset \mathbb{R}_{\geq 0} \times \mathbb{N}$ if, for each $(T, J) \in$ dom ϕ, dom $\phi \cap ([0, T] \times \{0, 1, ..., J\})$ is of the form $\bigcup_{j=0}^{J}([t_j, t_{j+1}] \times \{j\})$, with $0 = t_0 \leq t_1 \leq t_2 \leq t_{J+1}$. A solution ϕ is said to be *maximal* if it cannot be extended by a period of flow or a jump and *complete* if its domain is unbounded. A hybrid system is *well-posed* if it satisfies the hybrid basic conditions in (Goebel et al., 2012, Assumption 6.5).

4. PROBLEM STATEMENT AND HYBRID MODELING

The problem addressed in this paper is as follows:

Problem 1. Given system (1) and positive constants $0 < T^d \leq T_1^N \leq T_2^N$, design a hybrid algorithm including the hybrid observer in (4) with an associated clock synchronization scheme such that the resulting closed-loop system $\mathcal{H}$ is such that $\hat{z}(t, j) - z(t, j)$ converges to zero as $t + j \to \infty$.

To solve this problem, we employ the hybrid observer in (4), which requires finding a proper choice of the matrix L. The algorithm proposed in this paper also includes a synchronization scheme for the clocks that determine time

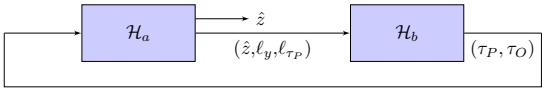

Fig. 3. Diagram of the observer and clock synchronization subsystem interconnection.

at both the plant and the observer. The details of the proposed hybrid algorithm are given in Section 4.1.

4.1 Hybrid Modeling

The hybrid model to solve Problem 1 is constructed such that the observer defined in (4) is recast with the dynamics of the network as a hybrid system with a set-valued jump map. Moreover, provisions are included to facilitate the inclusion of a clock synchronization strategy to ensure proper function of the hybrid observer. To build such a model, we treat the observer and clock synchronization strategy as individual but interconnected subsystems. Figure 3 describes such architecture, where $\mathcal{H}_a$ is the observer subsystem and $\mathcal{H}_b$ is the clock synchronization subsystem.

To model the aperiodic sampling, a timer variable τ_N is used. Between measurement sampling events the timer flows with dynamics given by $\dot{\tau}_N = -1$ and when $\tau_N = 0$, the state τ_N is reset to a value in the interval $[T_1^N, T_2^N]$. To model the transmission delay, an additional timer τ_δ with dynamics $\dot{\tau}_\delta = -q$ is used. Here $q \in \{0, 1\}$ is a discrete variable used to control the dynamics of τ_δ such that the timer is active only following measurement broadcast events. More precisely, $q = 1$ denotes an active measurement in the network and $q = 0$ denotes the absence of such a measurement in the network. Thus, when $\tau_N = 0$, τ_δ is reset to a point in the interval $[0, T^d]$ and q is reset to 1. When $\tau_\delta = 0$, indicating measurement arrival, τ_δ is reset to -1 and q is reset to 0. Having the timers τ_N and τ_δ defined in this way, with the addition of q, enforces the constraints defined in (2) for broadcast and arrival events. Additionally, we let ℓ_y and ℓ_{τ_P} represent memory states that define the plant measurement data and associated timestamp, respectively. The states τ_P and τ_O represents the global clocks for the respective plant and observer. The vector μ represents the state variables for a clock synchronization algorithm. Then, we define the state

$$x := (x_a, x_b) \in \mathcal{X}_a \times \mathcal{X}_b$$

where $x_a := (z, \hat{z}, \tau_N, \tau_\delta, q, \ell_y, \ell_{\tau_P}) \in \mathcal{X}_a$, $x_b := (\tau_P, \tau_O, \mu) \in \mathcal{X}_b$,

$$\mathcal{X}_a := \mathbb{R}^n \times \mathbb{R}^n \times [0, T_2^N] \times \big(\{-1\} \cup [0, T^d]\big) \times \{0, 1\} \times \mathbb{R}^m \times \mathbb{R}_{\geq 0}$$

$$\mathcal{X}_b := \mathbb{R}_{\geq 0} \times \mathbb{R}_{\geq 0} \times \mathcal{M}$$

and $\mathcal{M}$ is a closed set defining possible values of μ. The flow map is given by

$$F(x) = \begin{bmatrix} F_a(x_a) \\ F_b(\hat{z}, \ell_y, \ell_{\tau_P}, x_b) \end{bmatrix} \quad \forall x \in C$$

where

$$F_a(x_a) = \big(Az, A\hat{z}, 1, -q, 0, 0, 0\big)$$

and

$$F_b(\hat{z}, \ell_y, \ell_{\tau_P}, x_b) = \big(1, 1, F_s(\hat{z}, \ell_y, \ell_{\tau_P}, x_b)\big)$$

with F_s governing the continuous dynamics of μ. The flow set C is defined as $C := C_a \cap C_b$ where $C_a := C_{a_1} \cup C_{a_2}$ and

$$C_{a_1} := \{x \in \mathcal{X} : q = 0, \tau_N \in [0, T_2^N], \tau_\delta = -1\}$$
$$C_{a_2} := \{x \in \mathcal{X} : q = 1, \tau_\delta \in [0, T^d]\}$$

and C_b is the flow set defined by the clock synchronization algorithm. The jump map is given by

$$G(x) = \begin{bmatrix} G_a(x_a, \tau_P, \tau_O) \\ G_b(\hat{z}, \ell_y, \ell_{\tau_P}, x_b) \end{bmatrix} \quad \forall x \in D$$

where

$$G_a(x) = \begin{cases} G_1(x_a, \tau_P) & \text{if } x \in D_{a_1} \setminus D_b \\ G_2(x_a, \tau_O) & \text{if } x \in D_{a_2} \setminus D_b \\ x_a & \text{if } x \in D_b \setminus (D_{a_1} \cup D_{a_2}) \\ \{x_a, G_1(x_a, \tau_P)\} & \text{if } x \in D_{a_1} \cap D_b \\ \{x_a, G_2(x_a, \tau_O)\} & \text{if } x \in D_{a_2} \cap D_b \end{cases}$$

$$G_1(x_a, \tau_P) = \begin{bmatrix} z \\ \hat{z} \\ [T_1^N, T_2^N] \\ [0, T^d] \\ 1 \\ Mz \\ \tau_P \end{bmatrix} \quad G_2(x_a, \tau_O) = \begin{bmatrix} z \\ \hat{z}^\star \\ \tau_N \\ -1 \\ 0 \\ \ell_y \\ \ell_{\tau_P} \end{bmatrix}$$

where

$$\hat{z}^\star := \hat{z} + e^{A(\tau_O - \ell_{\tau_P})} L\big(\ell_y - M e^{-A(\tau_O - \ell_{\tau_P})} \hat{z}\big)$$

and

$$D_{a_1} = \{x \in \mathcal{X} : \tau_N = 0, q = 0\}$$
$$D_{a_2} = \{x \in \mathcal{X} : \tau_\delta = 0, q = 1\}$$

In the definitions above, G_b and D_b, respectively, define the jump map and jump set for the clock synchronization algorithm. The resulting jump set is

$$D = D_{a_1} \cup D_{a_1} \cup D_b$$

The hybrid system data (C, F, D, G) above define $\mathcal{H}$ as described in (5). With the chosen design of $\mathcal{H}$, the system can be viewed as the interconnection of two hybrid subsystems. Separating the clock synchronization from the system, one has a subsystem that is comprised only of the plant, observer, and network dynamics, denoted by $\mathcal{H}_a = (C_a, F_a, D_a, G_a)$. Conversely, the clock synchronization hybrid subsystem is denoted by $\mathcal{H}_b = (C_b, F_b, D_b, G_b)$.

Definition 4.1. Let $\mathcal{S}_\mathcal{H}$ represent the set of maximal solutions to $\mathcal{H}$. We say that a solution $\phi \in \mathcal{S}_\mathcal{H}$ is a *nominal* maximal solution if it belongs to the subset of maximal solutions defined by

$$\mathcal{S}_\mathcal{H}^{\text{nom}} := \big\{\phi \in \mathcal{S}_\mathcal{H} : \text{rge } \phi_{\tau_\delta} \subset \{0, -1\}\big\} \tag{6}$$

where ϕ_{τ_δ} is the τ_δ component of ϕ. Additionally, we say that a solution $\phi \in \mathcal{S}_\mathcal{H}$ is a *delay* maximal solution if it belongs to the subset of maximal solutions defined by $\mathcal{S}_\mathcal{H}^\delta := \mathcal{S}_\mathcal{H} \setminus \mathcal{S}_\mathcal{H}^{\text{nom}}$.

Qualitatively, one can interpret solutions belonging to $\mathcal{S}_\mathcal{H}^{\text{nom}}$ as a representation of the scenario where the measurements are free of transmission delays. For a given $\phi \in \mathcal{S}_\mathcal{H}$, when the timer τ_N expires (i.e., $\tau_N = 0$) the state jumps according to G_1. As a consequence of (6), the τ_δ component of the respective ϕ_{τ_δ} trajectory is mapped to 0 following the construction of G_1. Under such a scenario, observe that G_1 maps solutions to D_2, thus resulting in a subsequent jump according to G_2. In particular, there is no flow in between the two jumps.

Remark 4.2. Observe that Definition 4.1 applies to both $\mathcal{H}$ and $\mathcal{H}_a$, thus for the subsystem $\mathcal{H}_a$, we let $\mathcal{S}_{\mathcal{H}_a}^{\text{nom}}$ denote the set of nominal solutions to $\mathcal{H}_a$ and $\mathcal{S}_{\mathcal{H}_a}^\delta = \mathcal{S}_{\mathcal{H}_a} \setminus \mathcal{S}_{\mathcal{H}_a}^{\text{nom}}$ denote the set of delay solutions.

5. MAIN RESULTS

In this section, results guaranteeing convergence of the error $\varepsilon = z - \hat{z}$ to zero with the proposed algorithm are given. This is accomplished through a trajectory-based analysis to show convergence towards a set in which the system state and its estimate coincide. The results are broken into three parts. First, attractivity is shown for nominal solutions through a comparison to the exponentially converging trajectories given for the hybrid system in Ferrante et al. (2016). The result that follows utilizes a Lyapunov-like approach to compare the observer trajectories of a delay solution against those of a corresponding nominal solution. Finally, we present a result on the convergence of the error ε for the case where the plant and observer clocks are mismatched but eventually synchronize due to the presence of a clock synchronization algorithm. This last result is illustrated by Examples 6.1 and 6.2 featuring a widely used clock synchronization algorithm, the IEEE 1588 protocol, see IEEE (2008) for details.

5.1 Attractivity for nominal solutions

Starting with the attractivity for nominal solutions, in the result that follows, we show that the nominal solutions to $\mathcal{H}_a$ are such that the estimation error converges to zero. We prove this claim by showing that the trajectories of $\hat{z}$ for $\mathcal{H}_a$ are equivalent to the hybrid model presented in Ferrante et al. (2016) for a given set of parameters and initial conditions. To this end, let us consider the hybrid system in Ferrante et al. (2016) written in plant-observer coordinates, $x_r := (z, \hat{z}, \tau_N) \in \mathbb{R}^{2n} \times \mathbb{R}_{\geq 0}$

$$F^r(x_r) = \begin{bmatrix} Az \\ A\hat{z} \\ -1 \end{bmatrix} \quad G^r(x_r) = \begin{bmatrix} z \\ \hat{z} + LM(z - \hat{z}) \\ [T_1^N, T_2^N] \end{bmatrix}$$

$$C^r = \{(z, \hat{z}, \tau) \in \mathbb{R}^n \times \mathbb{R}^n \times \mathbb{R}_{\geq 0} : \tau_N \in [0, T_2^N]\}$$
$$D^r = \{(z, \hat{z}, \tau) \in \mathbb{R}^n \times \mathbb{R}^n \times \mathbb{R}_{\geq 0} : \tau_N = 0\}$$

leading to $\mathcal{H}^r = (C^r, F^r, D^r, G^r)$

The following property holds for $\mathcal{H}^r$.

Proposition 5.1. Let the matrix L be such that the set $\mathcal{A}_r := \big\{(z, \hat{z}, \tau_N) \in \mathbb{R}^n \times \mathbb{R}^n \times [0, T_2^N] : z = \hat{z}, \tau_N \in [0, T_2^N]\big\}$ *is globally attractive for $\mathcal{H}^r$. Then, the set*

$$\mathcal{A}_a := \mathcal{A}_r \times \big(\{-1\} \cup [0, T^d]\big) \times \{0, 1\} \times \mathbb{R}^m \times \mathbb{R}_{\geq 0} \tag{7}$$

is globally attractive for the hybrid system $\mathcal{H}_a$ for $T^d = 0$ with inputs $\phi_{\tau_P} \equiv \phi_{\tau_O}$.

Results for the design of L that guarantee the property in Proposition 5.1 are given in Ferrante et al. (2016).

5.2 Attractivity for delay solutions w/ synchronized clocks

Proposition 5.1 allows for a trajectory based comparison to be made between nominal and delay type solutions through a trajectory-based approach using a Lyapunov-like function. Consider the function from Ferrante et al. (2016) defined for every $x_a \in \mathbb{R}^n \times \mathbb{R}_{\geq 0}$ as

$$V(x_a) = \varepsilon^\mathsf{T} e^{A^\mathsf{T} \tau_N} P e^{A \tau_N} \varepsilon$$

where $\varepsilon = z - \hat{z}$ and $P = P^\mathsf{T} \succ 0$. Moreover, if

$$(\mathbf{I}-LM)^\mathsf{T} e^{A^\mathsf{T} v} P e^{Av}(\mathbf{I}-LM) - P \prec 0 \quad \forall v \in [T_1^N, T_2^N] \tag{8}$$

holds for given matrices L and P then global exponential stability of $\mathcal{A}_r$ for $\mathcal{H}^r$ is guaranteed; see Ferrante et al. (2016). Then, any $\phi_a^\delta \in S_{\mathcal{H}^\delta}(C_a \cup D_a)$ and $\phi_a^{\text{nom}} \in S_{\mathcal{H}^{\text{nom}}}(C_a \cup D_a)$ converge to the set $\mathcal{A}_a$ in (7). More formally, we have the following result.

Theorem 5.1. Given constants $T_1^N < T_2^N$ and matrices L and P such that condition (8) holds, then for each $T^d \in [0, T_1^N]$ the set $\mathcal{A}_a$ is attractive for the hybrid system $\mathcal{H}_a$ with inputs $\phi_{\tau_P} \equiv \phi_{\tau_O}$. In particular, for some positive constants α and β, each $\phi_a^\delta \in \mathcal{S}_{\mathcal{H}_a}^\delta$ with inputs $\phi_{\tau_P} \equiv \phi_{\tau_O}$ satisfies

$$\begin{aligned}\alpha|\phi_a^\delta(t,j)|_{\mathcal{A}_a} \leq V\big(\phi_a^\delta(t,j)\big) \leq & V\big(\phi^{\text{nom}}(t, s_\phi(j))\big) \\ & + \beta \varepsilon^{\text{nom}}(t,j)^\mathsf{T} \varepsilon^{\text{nom}}(t,j)\end{aligned} \tag{9}$$

for each $(t,j) \in \text{dom}\, \phi_a^\delta$ for associated ϕ^{nom}.

5.3 Attractivity for delay solutions with mismatched clocks

In this next result, we consider the case where the clock inputs τ_P and τ_O are mismatched, but eventually synchronize due to a finite time clock synchronization algorithm (like the one in Example 6.1). Before presenting the result, we introduce the following property that is required by the clock synchronization algorithm.

Assumption 5.2. For each ϕ to $\mathcal{H}$ there exists $T^* \geq 0$ such that $\lim_{t+j \nearrow T^*} |\phi_{\tau_P}(t,j) - \phi_{\tau_O}(t,j)| = 0$ and $|\phi_{\tau_P}(t,j) - \phi_{\tau_O}(t,j)| = 0$ for all $(t,j) \in \text{dom}\, \phi, t + j \geq T^*$.

We are ready to present our main result.

Theorem 5.2. Let Assumption 5.2 hold and every maximal solution to $\mathcal{H}_b$ is complete. Moreover, assume matrices L and P are such that (8) holds. Then, the closed set $\mathcal{A} := \mathcal{A}_a \times \mathcal{A}_b$ is globally attractive for $\mathcal{H}$ where $\mathcal{A}_b := \mathbb{R}_{\geq 0} \times \mathbb{R}_{\geq 0} \times \mathcal{M}$.

6. EXAMPLES

Example 6.1. In this example we present results for finite time convergence of the clock synchronization algorithm. Since, the synchronization algorithm depends solely on the reduced state vector x_b, consider the reduced hybrid system $\mathcal{H}_b$, restated here

$$\mathcal{H}_b \begin{cases} \dot{x}_b = F_b(x_b) & x_b \in C_b \\ x_b^+ \in G_b(x_b) & x_b \in D_b \end{cases}$$

and the closed set $\mathcal{A}_b := \{x_b : \tau_P = \tau_O\}$. Given the reduced state vector x_b with associated flow and jump maps F and G, the included vector μ allows for the implementation of various clock synchronization schemes to be considered for system analysis. In this section, we will present how the *IEEE 1558 Precision Clock Synchronization Protocol for Networked Measurement and Control Systems* Hetel et al. (2017) is modeled and incorporated into the system as an example. Per the standards of the protocol, we have the following assumptions:

- One-step clock nodes, that is clock nodes that generate and broadcast timestamps in one step.
- A dedicated communication channel between nodes with a fixed symmetrical transit time d.
- A fixed residence time c, representing the duration of time for a node to respond to a protocol message.

The residence and transit times affecting the clocks nodes at the plant (master) and observer (slave) are captured by two timers, τ_M and τ_S, respectively. Vectors m and s represent memory buffers to store the received and transmitted timestamps for the respective master and slave nodes. In addition, two discrete variables p and n are used to track the protocol state and set the dynamics of the node timers respectively. Finally, a timer τ_t is used to periodically initialize and start the synchronization protocol. Then, μ can be defined as $\mu := (\tau_t, \tau_M, \tau_S, m, s, p, n) \in \mathcal{M}$ where $\mathcal{M} := [0, T^*] \times [0, d] \times [0, d] \times \mathbb{R}^6 \times \mathbb{R}^6 \times \{0,1,2,3,4,5\} \times \{0,1,2\}$ We assume the transit time d to be larger than the residence time c, i.e., we assume the constraint $d > c$ in order to preserve the bounds of $\mathcal{M}$.

In order to prove convergence of $\mathcal{H}_b$ to $\mathcal{A}_b$, we utilize a trajectory-based approach to show that a solution $\phi \in \mathcal{S}_{\mathcal{H}_b}$, where $\mathcal{S}_{\mathcal{H}_b}$ is the set of solutions belonging to $\mathcal{H}_b$, converges to $\mathcal{A}_b$ in finite time. More formally, the result is:

Theorem 6.1. For each $\phi_b \in \mathcal{S}_{\mathcal{H}_b}$, there exists $T^* > 3d + 2c$ such that $|\phi(t,j)|_{\mathcal{A}_b} = 0$ for all $(t,j) \in \text{dom}\, \phi$ with $t + j \geq 2T^*$.

In light of this result, the IEEE protocol guarantees Assumption 5.2. The next example illustrates its use in our hybrid observer.

Example 6.2. Consider an oscillatory autonomous system given by $A = \begin{bmatrix} 0 & 1 \\ -1 & 0 \end{bmatrix}$ and matrix $M = [1\ 0]$ with timer bounds $T^d = T_1^N = 0.2$, $T_2^N = 1$. Using the design algorithm outlined in Ferrante et al. (2016) for the given parameters, the gain matrix is given by $L = [1.0097\ 0.6015]^\mathsf{T}$. Furthermore, let $T^* = 3$, $c = d = 0.5$. Starting with the case of synchronized clocks, i.e. $\phi(0,0) \in C_1 \cup D_1$ such that $\phi_{\tau_P}(0,0) = \phi_{\tau_O}(0,0)$, Figure 5 depicts the error in each state component for ϕ_a^{nom} and ϕ_a^δ. Figure 5 also shows the norm of the error for the two solutions, in addition the bound in (9) is plotted to demonstrate the asymptotic attractivity of ϕ_a^δ. The two trajectories flow together from the initial condition, at the first jump the error on the estimate for ϕ_a^{nom} decreases due to the measurement arrival at broadcast while ϕ_a^δ continues flowing. At the next jump the error for ϕ_a^δ decreases due to the arrival of the delay measurement and then resumes flowing with ϕ_a^{nom}. This behavior repeats until both solutions converge on the estimate.

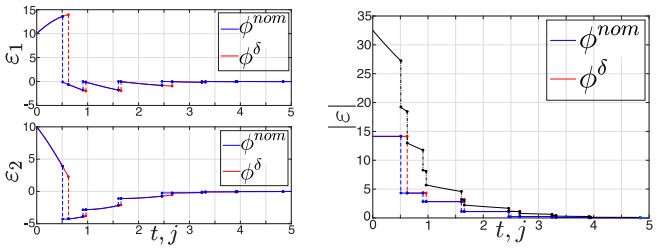

Fig. 5. Plot of state component errors (left) and error norm (right) of ϕ_a^{nom} and ϕ_a^δ for synchronized clocks with the bound (9).

Figure 4 presents the error norm trajectories for the case when the clock nodes are not synchronized, i.e., $\phi(0,0) \in C_1 \cup D_1$ such that $\phi_{\tau_P}(0,0) \neq \phi_{\tau_O}(0,0)$ but with the IEEE protocol present, for both ϕ_a^{nom} and ϕ_a^δ. In both figures, the

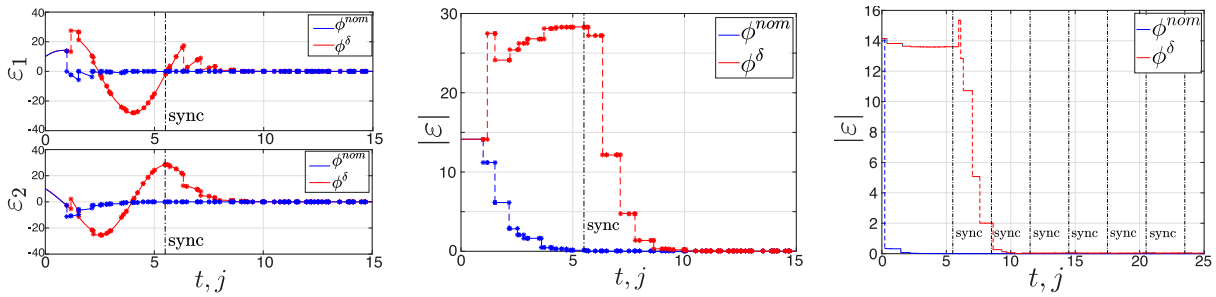

Fig. 4. Plot of the state component error (left) and error norm (center) for ϕ_a^{nom} and ϕ_a^{δ} for mismatched clocks τ_P and τ_O. Plot (right) gives the error norm for the case when τ_O drifts, the vertical lines marked `'sync'` indicate the instants when τ_P and τ_O synchronize.

trajectories flow together from the initial condition, at the first jump the estimate error for ϕ_a^{nom} decreases while ϕ_a^{δ} continues flowing. In the sequence of jumps that follow, the error norm of ϕ_a^{nom} converges to zero. The error norm of ϕ_a^{δ} however, increases until the clocks synchronize as marked by the dashed line denoted '*sync*'. In the jumps that follow the synchronization point, the error norm of ϕ_a^{δ} converges toward zero. Now consider the same system with a drifting observer clock, i.e., $\dot{\tau}_O = 1 + \gamma$ where $\gamma = 0.001$. In Figure 4, the error norm of the two trajectories for the simulation is given. Note the periodic synchronization of the plant and observer clocks prevents the drift in the observer clock from adversely affecting the norm of the error on the estimate for the delay solution. [1]

7. CONCLUSION

In this paper, we modeled an NCS with aperiodic sampling and network delays in a state estimation setting using the hybrid systems framework. We proposed an algorithm for state estimation with the inclusion of a clock synchronization scheme. Results for attractivity to a set of interest were given for the case of aperiodic sampling with and without network delays for both synchronized and mismatched clocks. Numerical simulations validating the results were also given.

REFERENCES

Cloosterman, M., van de Wouw, N., Heemels, M., and Nijmeijer, H. (2006). Robust stability of networked control systems with time-varying network-induced delays. In *Proceedings of the 45th IEEE Conference on Decision and Control*, 4980–4985.

Ferrante, F., Gouaisbaut, F., Sanfelice, R., and Tarbouriech, S. (2014). An observer with measurement-triggered jumps for linear systems with known input. volume 47, 140 – 145. 19th IFAC World Congress.

Ferrante, F., Gouaisbaut, F., Sanfelice, R.G., and Tarbouriech, S. (2016). State estimation of linear systems in the presence of sporadic measurements. *Automatica*, 73, 101 – 109.

Goebel, R., Sanfelice, R.G., and Teel, A.R. (2012). *Hybrid Dynamical Systems: Modeling, Stability, and Robustness*. Princeton University Press.

Hespanha, J.P., Naghshtabrizi, P., and Xu, Y. (2007). A survey of recent results in networked control systems. volume 95, 138–162.

Hetel, L., Fiter, C., Omran, H., Seuret, A., Fridman, E., Richard, J.P., and Niculescu, S.I. (2017). Recent developments on the stability of systems with aperiodic sampling: An overview. *Automatica*, 76, 309 – 335.

IEEE (2008). IEEE standard for a precision clock synchronization protocol for networked measurement and control systems. *IEEE Std 1588-2008*, 1–300.

Jungers, R.M., Kundu, A., and Heemels, W. (2017). Observability and controllability analysis of linear systems subject to data losses. IEEE.

Li, Y. and Sanfelice, R.G. (2013). A robust finite-time convergent hybrid observer for linear systems. In *52nd IEEE Conference on Decision and Control*, 3349–3354.

Luenberger, D. (1971). An introduction to observers. volume 16, 596–602.

Montestruque, L.A. and Antsaklis, P.J. (2003). On the model-based control of networked systems. volume 39, 1837 – 1843.

Naghshtabrizi, P. and Hespanha, J.P. (2011). *Implementation Considerations For Wireless Networked Control Systems*, 1–27. Springer New York, New York, NY.

Nesic, D. and Teel, A.R. (2004). Input-output stability properties of networked control systems. volume 49, 1650–1667.

Seiler, P. and Sengupta, R. (2001). Analysis of communication losses in vehicle control problems. In *Proceedings of the 2001 American Control Conference. (Cat. No.01CH37148)*, volume 2, 1491–1496.

Zhang, W., Branicky, M.S., and Phillips, S.M. (2001). Stability of networked control systems. volume 21, 84–99.

[1] Code at github.com/HybridSystemsLab/HybridObsPlanarPlant